IMPACT OF COMET SHOEMAKER-LEVY-9 ON JUPITER

Toshiko Takata, Thomas J. Ahrens, John D. O'Keefe

Lindhurst Laboratory of Experimental Geophysics, Seismological Laboratory 252-21, California Institute of Technology, Pasadena, CA 91125

and

Glenn S. Orton

Jet Propulsion Laboratory, Pasadena, CA 91109

Abstract

We have employed three-dimensional numerical simulations of the impact of Comet Shoemaker - Levy 9 (SL9) on Jupiter and the resulting vapor plume expansion using Smoothed Particle Hydrodynamics (SPH) method. An icy body with a diameter of 2 km can penetrate to an altitude of -350 km (0 km = 1 bar) and most of the incident kinetic energy is transferred to the atmosphere between -100 km to -250 km. This energy is converted to potential energy of the resulting gas plume. The unconfined plume expands vertically and has a peak radiative power approximately equal to the total radiation from Jupiter's disc. The plume rises a few tens of atmospheric scale heights in ~10^2 seconds. The rising plume reaches the altitude of ~3000 km, however, no atmospheric gas is accelerated to the escape velocity (~60 km/s).

INTRODUCTION

Fragments of Comet Shoemaker-Levy-9 (SL9) are predicted to impact Jupiter in July 1994 [Shoemaker et al., 1993; Yeomans and Chodos, 1993]. Observations using the Hubble Space Telescope indicate the maximum fragment diameters of ~4 km, and ~10 fragments are ~3 km in diameter [Weaver et al., 1993]. The total energy released to the Jovian atmosphere upon impact of all of the comet fragments (CF's) will be 10^{29} to 10^{31} erg.

ENTRY AND HYDRODYNAMIC INSTABILITIES

We have modeled the impact of CF's onto Jupiter and the resulting plume expansion using the Lagrangian method called Smoothed Particle Hydrodynamics (SPH) [Gingold and Monaghan, 1977]. A Tillotson equation of state for ice was used for the cometary material [O'Keefe and Ahrens, 1982] and an ideal gas with $\gamma = 1.4$ is employed for the atmosphere. We assume the atmospheric structure observed by Voyager and extend our model adiabatically into the interior of Jupiter. We performed calculations for two sizes of CF's, 2 and 10 km in diameter with an impact velocity of 60 km/s and impact angle of 40° from the zenith. Detailed description of our calculations is given in Takata et al. [1994]. These sizes characterize the range of maximum sizes and energy of the Comet SL9 fragments as perceived since discovery [Chapman, 1993a; Chapman, 1993b; Scotti and Melosh, 1993; Sekanina et al., 1993; Weaver et al., 1993].

When the bolide enters Jupiter's atmosphere it induces a high temperature shock wave in the gas in front of the bolide. The radiation and convective flow of the shocked atmosphere around the front melts and ablates material from the bolide. The high speed flow of the atmosphere tangential to the melted material drives surface-wave Kelvin-Helmholtz (K-H) instabilities that grow and shed melt droplets into the flow behind the body. These particles are micron-sized, as the fastest growing wavelengths of the K-H instabilities are microns in length. The relative mass loss for large impactors is small [Bronshten, 1983]. Wavelengths much shorter ~1 micron are suppressed by the viscosity of the melt and do not grow --this is seen in the turnover in the curves in Figure 1 calculated using the formulation of Keith and Banks [1990].

As the bolide penetrates further into the atmosphere, dynamic pressures within the shocked material in front of the bolide exceed the strength of the impactor. This results in fracture and then subsequent radical deformation of the bolide. The compression occurring during the passage of the fracturing wave is dependent upon R/ℓ, where R is bolide radius and ℓ is atmospheric scale height. The characteristic time scale of the process of fracture wave propagation is, $t_{fw} = 2R/U_S$, (see Figure 2a). The aerodynamic stresses acting on the bolide are greatest at the center of the

fragment and give rise to the spreading and flattening of the bolide [Melosh, 1989; Vickery, 1993; Zahnle, 1992; Zahnle and MacLow, 1994]. The relative diameter was found in SPH calculations to increase from unity to maximum of ~4 for a 1 km radius impactor and ~1.7 for a 5 km radius impactor (see Figure 2b). However, MacLow and Zahnle [1994] point out on the basis of calculations conducted by assuming the bolide acts as a precompressed ideal gas, that the present calculations (which yield motions similar to hydrodynamic instabilities) may be spatially unresolved and the above scale lengths may be too large. However, this type of distortion and flattening has been observed in laboratory experiments of breakup of liquid droplets by gas streams [Ranger and Nichols, 1970]. We infer that such hydrodynamic instabilities prevent the projectile from expanding to the effective diameters that are as large as ~20 times the undisturbed diameter predicted by models based only on inertial confinement [Zahnle, 1992].

Besides K-H instabilities, Rayleigh-Taylor (R-T) instabilities occur and these are driven by the deceleration of the bolide and by the aerodynamic forces acting near the center of the front of the bolide. The particles ejected in Figure 2a are believed to result from R-T instabilities. The time for R-T instabilities to grow relative to the characteristic deceleration time, t_{decel}, is given by:

$$t_{R-T} / t_{decel} = \{[R/(2\pi\ell f)](\lambda/R)\}^{1/2} \quad (1)$$

where

$$f = \ell n \{(2/(3C_d))(\rho_b R/(\rho_a \ell)\} \quad (2)$$

and λ is the instability wavelength, C_d the drag coefficient, ρ_a and ρ_b the densities of the atmosphere and bolide. Ivanov et al. [1992] observed that upon passage of impactor through the Venusian atmosphere that surface instabilities grow at the front of the projectile and limited the distortion of the projectile. Recently, Boslough et al. [1993] observed similar phenomena in their calculation of SL9 impact on Jupiter.

Instabilities are driven by velocity differences between the atmosphere and the bolide surface and are most prevalent near the edge of the front face of the bolide. The time for K-H instabilities to grow relative to the bolide characteristic deceleration time is given by

$$t_{K-H} / t_{decel} = \left(10/(\pi\sqrt{3})\right)\left(\eta_p/\eta_a\right)^{1/2}(R/\ell)^{2/3}(\lambda/R)\ (1/f) \quad (3)$$

where η_a and η_b are the viscosities of the atmosphere and the bolide.

The final breakup of the bolide occurs when the instabilities having wavelengths on the order of the size of the bolide ($\lambda/R \sim 1$) grow to large amplitudes. Referring to Figure 1, we see that growth rates for large scale K-H instabilities are on the order of 1 s^{-1} for bolides 1 km in radius and on the order of 10^1 s^{-1} for 1 to 5 km radius impactors. The growth rates for R-T instabilities are also comparable to these values. The present SPH calculations show disintegration occurring at time scales predicted from these growth rates (Figure 2). Shown in Figure 2c is final disintegration and the stopping of the disintegrated fragments.

We find that CF's can penetrate to an altitude of -350 km(~200 bar), in the case of an initial diameter, D = 2 km and to the altitude of -550 km (~800 bar), in the case of D = 10 km. The energy transfer from the CF to the atmosphere occurs mostly in the altitude range from -100 km (~10 bar) to -250 km (~100 bar) in the case of D = 2 km and -350 km (~200 bar) to -480 km (~500 bar) in the case of D = 10 km (Fig. 3).

THE ATMOSPHERIC PLUME

We subsequently carried out the calculation of a plume expansion (Fig. 4). We distributed ~10^5 atmospheric particles in model atmospheric box of 500 km width extending from 350 to -400 km altitude in the case of the CF of D = 2 km. The energy density of deposition shown in figure 3 is placed on atmospheric particles along the trajectory. In ~10^2 seconds after the impact, the fireball rises a few tens of atmospheric scale heights and the unconfined plume expands vertically rather than horizontally in an inhomogeneous atmosphere. Buoyancy forces result in the upward motion of the plume. Some 25% of the energy deposited in the deep atmosphere can be transported above 100 km in 10^2 seconds and most of the energy is brought up above 100 km in ~200 seconds. A mass of atmospheric gas equal to 10 times the CF mass is transported from below the cloud deck to above 1000 km in 10^2 seconds and a total of ~20 times the initial CF mass is elevated above 100 km. The rising plume achieves an altitude of ~3000 km, however, no atmospheric gas is accelerated to escape velocity. The plume transport results in the vertical mixing

of deep atmospheric constituents, such as NH_3, H_2O, and CH_4, in addition to the vaporized cometary materials. Subsequent condensation of both deep atmospheric and cometary materials may be a source of dust condensates in the upper atmosphere.

RADIATIVE SIGNATURES

The radiation upon entry from the heated atmosphere and vaporized cometary media within the temporary conical cavity will be multiply Rayleigh scattered by the H_2 and He of Jupiter's atmosphere, and obscured by the several Jovian cloud decks. Moreover, the radiant flux may also be reflected from one or more Galilean satellites depending upon their position during impact. The observed color temperature during entry of a cometary fragment into Jupiter's atmosphere will be in excess of 10^4 K. The details of the spectrum will depend on the degree of ionization which occurs in the bolide material and in Jupiter's atmosphere [Chevalier and Sarazin, 1994; Zahnle and MacLow, 1994]. In any case, the ~10^4 K temperature seen in the impact flash during bolide entry will occur (because of radiative cooling) for only a minute or so.

Because the optical radiation from the (~10sec) entry of a SL9 fragment into Jupiter will emit radiation anisotropically , we chose to model only the radiation from the second SPH calculation describing the plume. Moreover, the entry flash may be partially obscured in many directions by the asymmetry of the entry hole, opacity of ionized gas, and the NH_3, NH_4SH, and H_2O cloud layers.

Starting with plume calculations of 2-and 10-km SL9 fragments, we have considered each particle as a greybody radiator disc and calculated the total normal radiative power as a function of wavelength at a series of times (e.g. Figure 5). Since we are not accounting for the absorption of CH_4 or Rayleigh scattering from H_2, the present calculations are an upperbound to the actual radiating power. However, most of the hot materials, shown in Figure 4 are at, or above, the elevations such that there will be minimal absorption effects of clouds. We observe that in the case of the 2 km comet nucleus fragment impact that its particle velocity is such that it should achieve an altitude of 3000 km within several minutes.

PREDICTIONS

In July 1994, the Galileo spacecraft will be in a good position (1.6 AU away from Jupiter) to observe with the Solid State Imaging Experiment [Russell, 1992] the plumes from SL9 fragment collisions directly. The flux emitted by the plume associated with a 2-km diameter fragment is some 30% of the solar visible flux reflected by Jupiter. It is comparable to both Jupiter's reflected solar flux near 1 micron and an order of magnitude or more higher than Jupiter's near-infrared reflected flux, and Jupiter's average 5- and 7.8-micron thermal emission. Using our 2-and 10-km results, we infer that the plume from impact of a 2-km diameter fragment yields a radiant power equivalent to 3% of Jupiter's total flux and some 10% of Jupiter's average thermal emission at 5 and 7.8 microns. Thus, observations by Galileo instruments are technically feasible for a large number of the fragments if they are as dense as we have assumed.

Direct earth-based observations of the impact-induced plume may be possible as it rises above Jupiter's horizon as seen from the earth (prior to dawn at the impact point). However, observation of the inner Galilean satellites brightnesses as a function of time may detect a reflection of the plume illumination superimposed on the solar illumination. The plume generated by a 1-km diameter fragment would increase Io's visible flux by some 10% in the visible and by 1% or less in the near infrared. The plume generated by the 0.5-km fragment illuminates Io only 0.01-0.03% more than the sun between the visible and near infrared. However, at wavelengths of 5 microns and longer, the 0.5 km fragment induced plume illuminates Io some 1-3% more than the sun. Clearly, them most favorable spectral band for indirect detection of impart-induced plumes is in the near or middle infrared.

For SL9 fragments with diameters <1 km, impact-induced plume brightnesses are expected to be decreased by plume and atmospheric opacity effects [Chevalier and Sarazin, 1994]. In these cases, the wavelength of peak spectral power is likely to be diagnostic of fragment size. Our present study indicated the wavelength of maximum plume intensity, λ_m, and fragment diameter, D, are related by the Wein's law type relation: $\lambda_m D^3 \simeq 5 \times 10^{11}$ cm^4.

ACKNOWLEDGMENTS

D. Stevenson, J. Spencer, K. Zahnle, T. Johnson, and G. Ravichandran provided many helpful suggestions which we appreciate. We thank K. Zahnle and M. MacLow, and G. Field and A. Ferrara for their preprints, and P. Weissman, M. A'Hearn, and K. Ziemelis for critical comments. Research supported by NASA and Cray Research Corp. Contribution number 5381, Division of Geological and Planetary Sciences.

Fig 1 Growth rate of Kelvin-Helmholtz instabilities as a function of the diameter of the impactor divided by the instability wave length. The curves are for impactor diameters of 1, 2, and 10 km and the depth into the atmosphere is 300 km relative to the 1 bar level of Jupiter.

Fig. 2. Smoothed-Particle -Hydrodynamic (SPH) calculations of the penetration of a fragment of Comet Shoemaker-Levy-9 fragment into Jupiter's atmosphere. The diameter of the bolide is 10 km and the angle of entry is 40° from the zenith. Shown are the density fields at various times relative to the time the bolide penetrated to the 1 bar altitude. Dots indicate planetary atmosphere and triangles bolide SPH particles. The times are 2.0 , 5.0, and 21 sec., respectively .

Fig. 3. The fractional energy deposition of the initial kinetic energy of the comet as a function altitude in the case of 2 and 10 km diameter-cometary fragments. The results of SPH calculation are shown by the solid lines, and the results of meteoric ablation model with the ablation coefficients, σ, of 10^{-9} and $10^{-8} s^2/m^2$ [Bronshten, 1983] for D = 10 km, are shown by dashed lines.

Fig. 4. The pressure of atmospheric particles upon plume expansion of D = 2 km cometary fragment after 75.2 sec (after Ahrens et al. [1994]).

Fig. 5 Calculated spectra from Shoemaker-Levy-9 impact-induced plumes for 2 and 10 km diameter fragments. The peak power from the 2 km fragments radiates at the approximately same power level as the total Jupiter disk. The total power from the sun, considered as a point source is shown, for comparison.

REFERENCES

Ahrens, T. J., T. Takata, J. D. O'Keefe, and G. S. Orton, Comet Shoemaker-Levy-9 impact on Jupiter, *Nature*, submitted, 1994.

Boslough, M. B., D. A. Crawford, M. E. Kipp, T. G. Trucano, and J. M. McGlaun, Simulations of cometary interaction with Jupiter: Preliminary 2D and 3D calculations of the sensitivity of the event to bolide representation and angle of incidence (abstract), *Bull. Am. Astron. Soc.*, *25*, 1045, 1993.

Bronshten, V. A., *Physics of Meteoric Phenomena*, pp. 1-356 pp., D. Reidel Publishing Co., Boston, 1983.

Chapman, C. R., Comet on target for Jupiter, *Nature*, *363*, 492-493, 1993a.

Chapman, C. R., Preparing for the comet crash, *Nature*, *365*, 784-785, 1993b.

Chevalier, R. A., and C. L. Sarazin, Explosions of infalling comets in Jupiter's atmosphere, *Astrophys. J.*, in press, 1994.

Gingold, R. A., and J. J. Monaghan, Smoothed particle hydrodynamics: theory and application to non-spherical stars, *Month. Not. R. Astr. Soc.*, *181*, 375-389, 1977.

Ivanov, B. A., I. V. Nemchinov, V. A. Svetsov, A. A. Provalov, V. M. Khazins, and R. J. Phillips, Impact cratering on Venus: Physical and mechanical models, *J. Geophys. Res.*, *97*, 16,167-16,182, 1992.

Keith, J. C., and N. E. Banks, Hypervelocity impact and aerodynamic breakup of liquids, *Int.. J. Impact Engng.*, *10*, 309-322, 1990.

MacLow, M.-M., and K. Zahnle, Explosion of Comet Shoemaker-Levy-9 on entry into the Jovian atmosphere, *Nature*, submitted, 1994.

Melosh, H. J., *Impact Cratering, A Geologic Process*, pp. 1-245, Oxford University Press, New York, 1989.

O'Keefe, J. D., and T. J. Ahrens, Cometary and meteorite swarm impact on planetary surfaces, *J. Geophys. Res.*, *87*, 6668-6680, 1982.

Ranger, A. A., and J. A. Nichols, Shape and surrounding flow field of a drop in a high-speed gas stream, *AIAA Journal*, *8*, 1720-1722, 1970.

Russell, C. T., (Ed.), Special Issue, Galileo Instruments, *Space Science Reviews*, *60*, [1-4], 413-590, 1992.

Scotti, J. V., and H. J. Melosh, Tidal breakup and dispersion of P/Shoemaker-Levy 9: Estimate of progenitor size, *Nature*, *365*, 7333, 1993.

Sekanina, Z., P. W. Chodos, and D. K. Yeomans, Tidal disruption and the appearance of periodic Comet-Shoemaker-Levy-9, *Astron. J.*, submitted, 1993.

Shoemaker, C. S., E. M. Shoemaker, and D. H. Levy, Comet Shoemaker-Levy, *IAU Circ.*, *5725*, 1993.

Takata, T., T. J. Ahrens, G. S. Orton, and J. D. O'Keefe, Comet Shoemaker-Levy-9, Impact on Jupiter --- Disintegration and the resulting plume evolution, *Icarus*, submitted, 1994.

Vickery, A., Numerical simulation of a comet impact on Jupiter, *EOS*, *74*, 391, 1993.

Weaver, H. A., P. D. Feldman, M. F. A'hearn, C. Arpigney, R. A. Brown, E. F. Helin, D. H. Levy, B. G. Marsden, K. J. Meech, S. M. Larson, K. S. Noll, J. V. Scotti, Z. Sekanina, C. S. Shoemaker, E. M. Shoemaker, T. E. Smith, A. D. Storrs, D. K. Yeomans, and B. Zellner, HST observations of Comet Shoemaker-Levy (Abstract), *Bull. Am. Astron. Soc.*, *25*, 1042, 1993.

Yeomans, D. K., and P. Chodos, *Minor Planet Circ. No.*, *22197*, 1993.

Zahnle, K., Airburst origin of dark shadows on Venus, *J. Geophys. Res.*, *97*, 10243-10255, 1992.

Zahnle, K., and M.-M. MacLow, The collision of Jupiter and Comet Shoemaker-Levy-9, *Icarus*, in press, 1994.

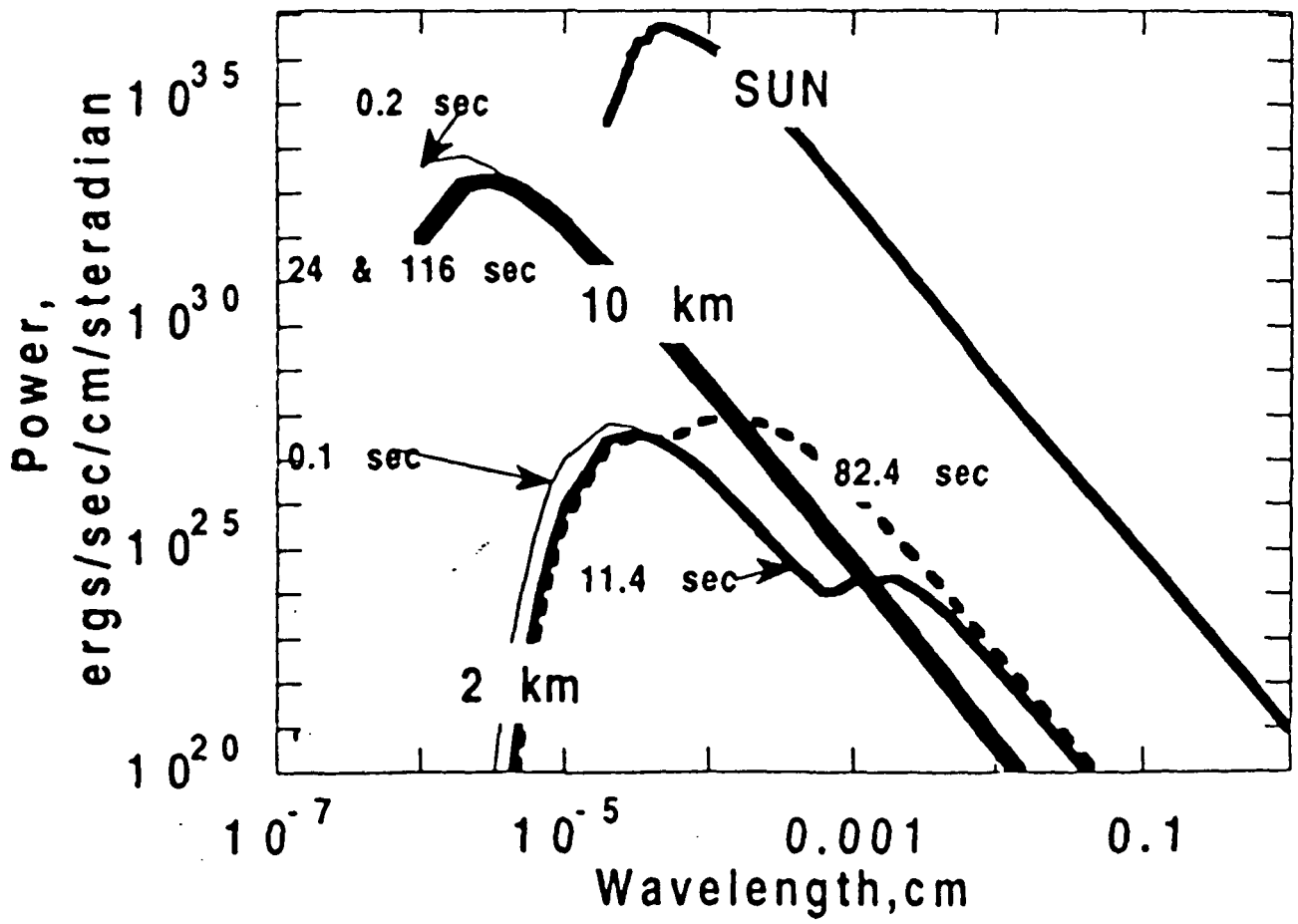

TJA94004SFD

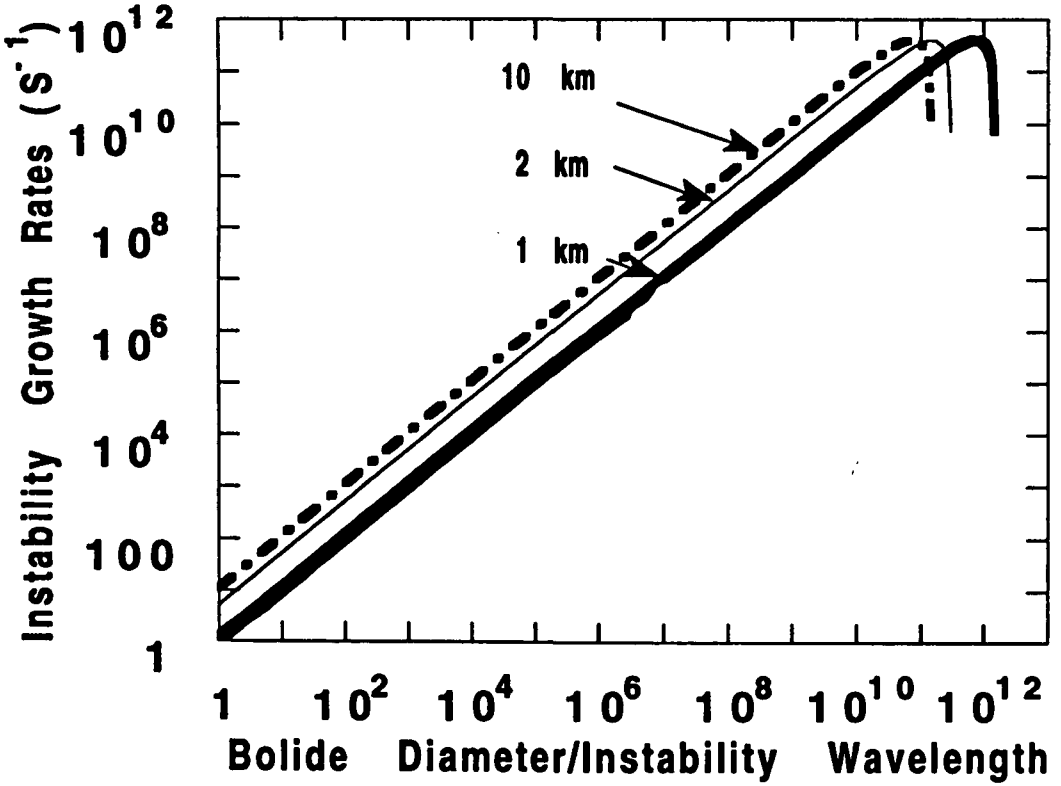

TJA94003SFD

TJA94008SFD

2

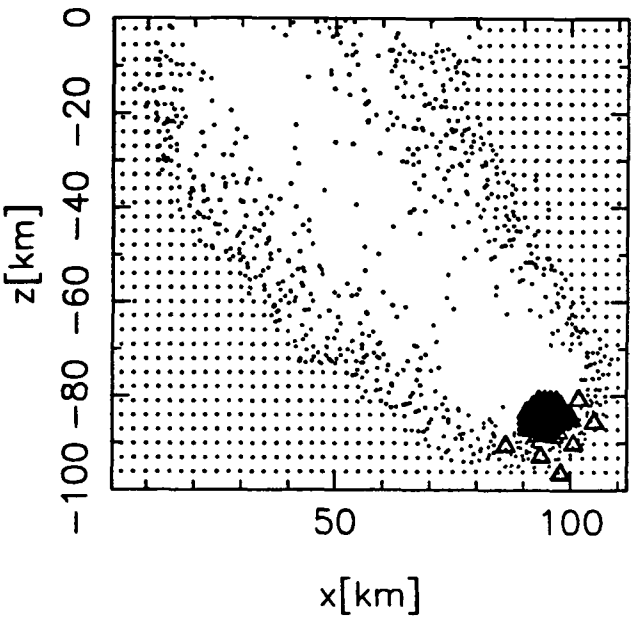
z[km]
0
−20
−40
−60
−80
−100
50
100
x[km]

(a)

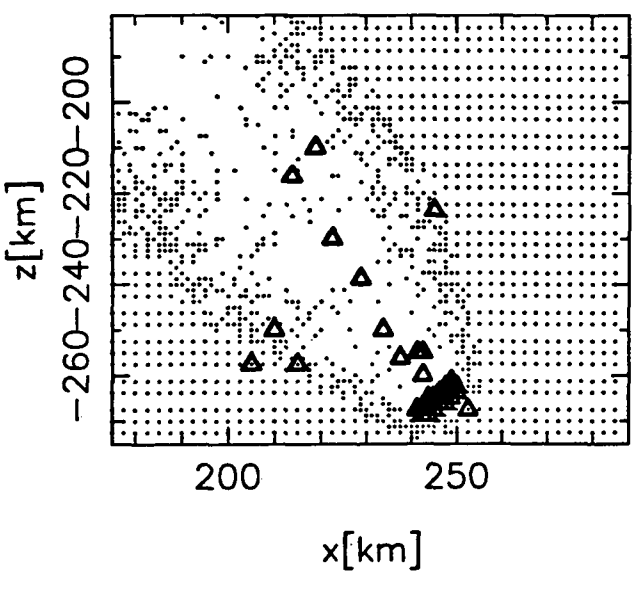
z[km]
−200
−220
−240
−260
200
250
x[km]

(b)

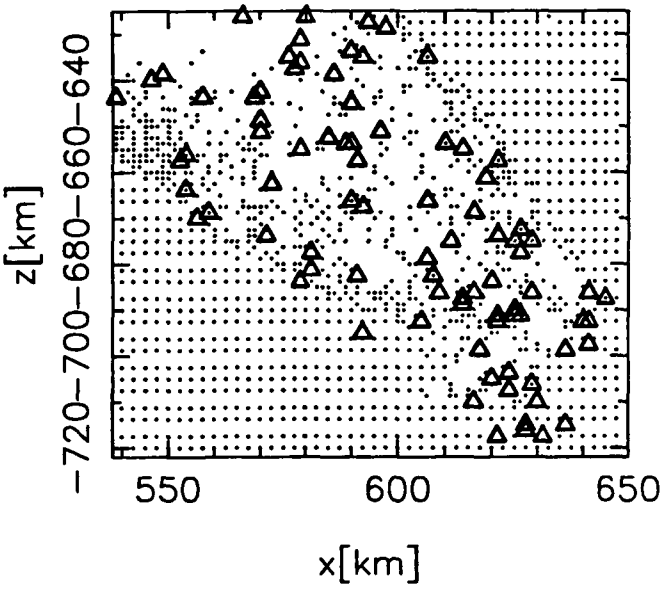
z[km]
−640
−660
−680
−700
−720
550
600
650
x[km]

(c)

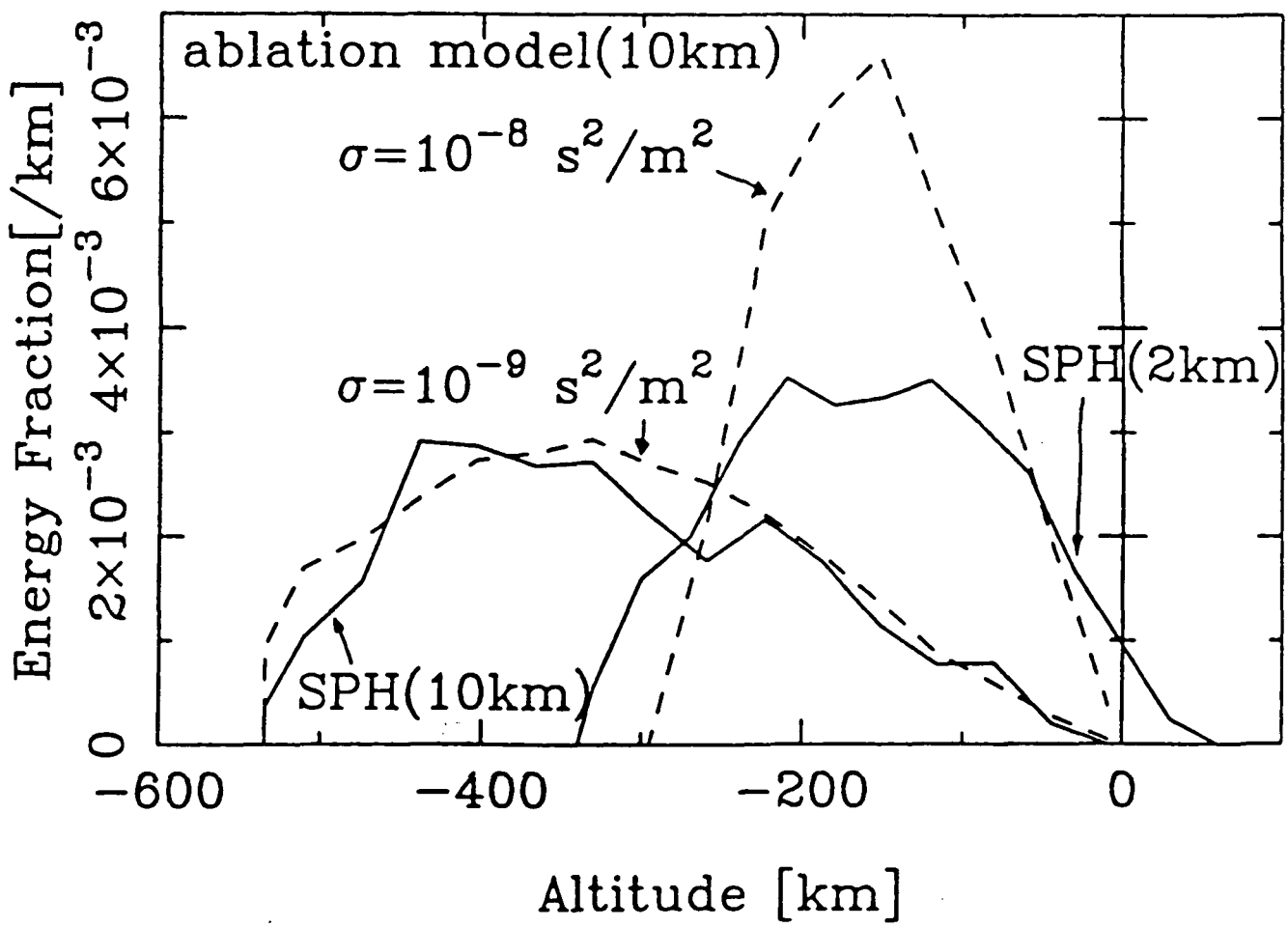
ablation model(10km)
σ=10⁻⁸ s²/m²
σ=10⁻⁹ s²/m²
SPH(2km)
SPH(10km)
Energy Fraction[/km]
0
2×10⁻³
4×10⁻³
6×10⁻³
−600
−400
−200
0
Altitude [km]

Pressure : t = 75.2 [s]